# Influence of Radiative Heat Transfer on Growth Temperature during Epitaxy of HgCdTe Layers

© V.A. Shvets<sup>1</sup>, D.V. Marin<sup>2,3</sup>, I.A. Azarov<sup>1</sup>, M.V. Yakushev<sup>1</sup>

630090 Novosibirsk, Russia

<sup>3</sup> Specialized Educational Scientific Center of Novosibirsk State University,

630090 Novosibirsk, Russia

E-mail: basil5353@mail.ru Received April 29, 2025 Revised July 4, 2025 Accepted July 4, 2025

There are two mechanisms of substrate heating during molecular beam epitaxy: thermal conductivity and thermal radiation. The paper considers the contribution of radiative heating to establishing the sample temperature during epitaxy of the CdHgTe layer. At the initial stage of growth, the emissivity of the structure changes and the thermal balance is disturbed. Numerical calculations have shown that in the absence of thermal contact between the sample and the heater, this should lead to a significant increase in the equilibrium temperature of the structure. The dynamics of temperature change during continuous growth of the CdHgTe layer is calculated. It follows from these calculations that a residual change in temperature will also be observed after the growth has ceased. Experiments performed with use of spectral ellipsometer did not reveal the expected temperature changes. From this it was concluded that in installations of the "Ob" type, when the sample is in mechanical contact with a heated graphite washer, the radiative heating mechanism is not dominant.

**Keywords:** radiative heating, absorption spectrum, growth surface temperature, thermal contact, cadmium-mercury-telluride, ellipsometry.

DOI: 10.61011/SC.2025.03.61559.7916

## 1. Introduction

When growing CdHgTe layers by molecular beam epitaxy (MBE), it is necessary to maintain a number of technological parameters with high accuracy. For instance, it is reported in Refs. [1,2] that the temperature range for obtaining defect-free layers of CdHgTe is several degrees. Thermocouple temperature control for the substrate in layer growth plants is not possible for a number of reasons. Firstly, due to the technical features of the installation, it is impossible to ensure thermal contact of the thermocouple junction with the substrate. Secondly, in the absence of reliable thermal contact of the substrate with the carrier, the junction of the thermocouple is an additional channel of heat removal and can distort the temperature field in the contact area. Therefore, various non-contact methods are used for temperature control [3,4], including spectral ellipsometry [5,6].

At the initial stage of epitaxy of narrow-band semiconductors, including CdHgTe, the balance of heat fluxes incident on the substrate and emitted by it changes dramatically due to changes in the emissivity of the sample. This, in turn, leads to the establishment of a new equilibrium of heat fluxes and the establishment of a new equilibrium temperature. The crucial point in this case is the presence or absence of thermal contact between the substrate and the heater. For instance, the substrate touches the metal

holder only along the perimeter in "Riber" installations. When performing studies, the substrate is glued to a massive holder with indium or gallium [7]. The thermal contact of the substrate with the molybdenum holder is provided in Ref. [4] by a specially developed graphite paste.

In the molecular beam epitaxy unit "Ob" the heating of the working area is carried out by thermal radiation from the heater. In this case, the sample itself (a silicon substrate with a CdTe film) is pressed against the perimeter of the holder by a graphite washer located in close proximity to the heater. This design allows the sample to be heated both by radiation from a graphite washer and by thermal conductivity. The relative contribution of both heating mechanisms depends on the absorbency of the substrate and its thermal contact with the graphite washer and holder. Two limiting cases can be considered.

If the thermal contact is good enough to provide preferential heating compared to radiation, then the sample will have the temperature of the heated washer, and it will not undergo drastic changes due to the high heat capacity of the washer. If the thermal contact is weak, then thermal radiation will be the dominant mechanism of heat transfer, and this can lead to a change in the temperature of the sample at the initial stage of growth of CdHgTe. Each fixed layer thickness will have its own equilibrium temperature. With continuous growth of the layer, the temperature will change following the change in thickness. A change in

3 145

<sup>&</sup>lt;sup>1</sup> Rzhanov Institute of Semiconductor Physics, Siberian Branch, Russian Academy of Sciences, 630090 Novosibirsk, Russia

<sup>&</sup>lt;sup>2</sup> Novosibirsk State University,

temperature, in turn, can affect the kinetics of growth reactions, as it leads to a change in the concentration of mercury on the surface [8], can shift the kinetic equilibrium of reactions and change the composition of the growing layer of CdHgTe [9].

The question of what contribution each of the considered heating mechanisms makes with an growth in CdHgTe is extremely important and remains open. Thus, it was experimentally shown in Ref. [10] that radiation is the main mechanism for a GaAs substrate with a wide absorption band in the IR range. However, for silicon, which has a narrow phonon absorption peak at IR, the situation may be reversed.

It is not possible to quantify the dynamics of temperature changes, since it is difficult to take into account many uncontrolled parameters that determine the contribution of both mechanisms. However, it is possible to consider the limiting case when heating is carried out only by radiation, and there is no thermal contact of the substrate with the elements of the chamber. Within the framework of this assumption, it is possible to carry out estimated calculations of temperature dynamics and compare them with experiment. This would allow answering the question about the determining mechanism of heating.

The purpose of this work is to numerically evaluate possible changes in the substrate temperature during radiative heat exchange due to the appearance of a narrow-band layer of CdHgTe, and experimentally verify which heating mechanism of the sample is dominant in the growth plants used.

#### 2. Radiative heat transfer model

Let us consider the limiting case when the sample is heated only by thermal radiation. For calculations, we will use the one-dimensional model shown in Figure 1. The substrate S is heated by radiation from a graphite washer G with a set temperature  $T_G$  located in the immediate vicinity of the sample. The thermal radiation of all other elements of the vacuum chamber is taken into account by defining a plane VC with a blackbody emissivity and a temperature  $T_{VC}$ . The Si/CdTe/HgCdTe sample faces the silicon side towards the heater (boundary 12) and the epitaxial layers towards the plane VC (boundary 10). The condition for the balance of heat fluxes for a sample with a temperature of  $T_S$  has the following form:

$$q_G + q_{VC} = q_{12} + q_{10}, (1)$$

where  $q_G = \int r(T_G, \lambda) A_{12} d\lambda$  and  $q_{VC} = \int r(T_{VC}, \lambda) A_{10} d\lambda$  are the heat fluxes absorbed by the sample from the heater and chamber, respectively, and  $q_{12} = \int r(T_S, \lambda) A_{12} d\lambda$  and  $q_{10} = \int r(T_S, \lambda) A_{10} d\lambda$  are the heat fluxes radiated by sample surfaces,  $r(T, \lambda)$  is the spectral density of blackbody radiation determined by Planck's formula:

$$r(T, \lambda) = \frac{\text{const}}{\lambda^5} \cdot \frac{1}{\exp(\frac{hc}{\lambda kT}) - 1},$$
 (2)

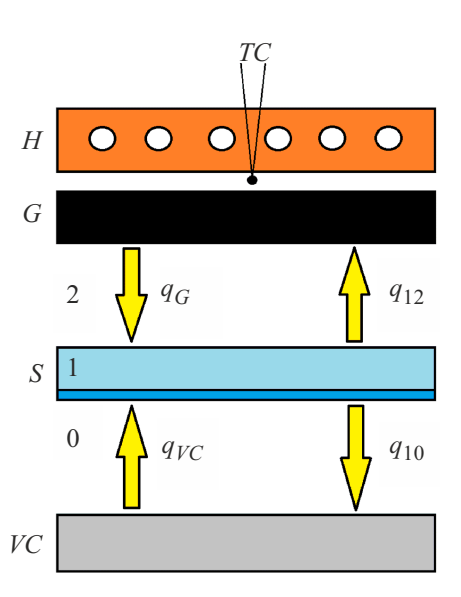


**Figure 1.** Schematic representation of the heat exchange model between the sample and the surrounding elements of the vacuum chamber: H — heater, TC — thermocouple, G — graphite washer heated to temperature  $T_G$ , S — sample, VC — surface describing the thermal radiation of a vacuum chamber.

 $A_{12}$  and  $A_{10}$  is the emissivity (absorption) of the cor-Their values were found responding sample surfaces. from the conditions [11]  $A_{1j} + T_{1j} + R_{1j} = 1$ , (j = 0, 2), where  $T_{1j}$  and  $R_{1j}$  are the energy transmission and reflection coefficients for the surfaces under consideration. The coefficients  $T_{1j}$  and  $R_{1j}$  were calculated using the matrix method [12], which took into account interference on the CdTe and CdHgTe layers. The rays reflected repeatedly from the edges of the silicon wafer were stacked in intensity due to the large thickness of the wafer compared to the coherence length of the radiation. The spectra of optical permanent materials required for these calculations were taken at room temperature from Refs. [13,14]. At the same time, the temperature shift of the absorption edge was taken into account for CdHgTe [15]. Figure 2 shows the absorption spectra of silicon and CdHgTe (x = 0.2), as well as the Planck contour, graphite washer temperatures of  $T_G = 550 \,\mathrm{K}$ . From a comparison of the characteristics shown in the figure, we see that the thermal radiation can be absorbed in the Si/CdTe/CdHgTe structure in the long-wavelength region of intrinsic absorption of CdHgTe  $(2-6\,\mu\text{m})$ , as well as in the region of phonon absorption of silicon of  $10-25 \mu m$ . Cadmium telluride also has a wide band of phonon absorption with a maximum near  $70 \,\mu\text{m}$ , but its integral contribution to the heating of the substrate is 2 orders of magnitude less than from absorption on silicon due to the insignificant thickness of the CdTe layer and the rapid decay of the Planck function with increasing wavelength. Therefore, in the future, the integration of thermal radiation was carried out in the spectral range from 0.5 to  $25 \,\mu\text{m}$ .

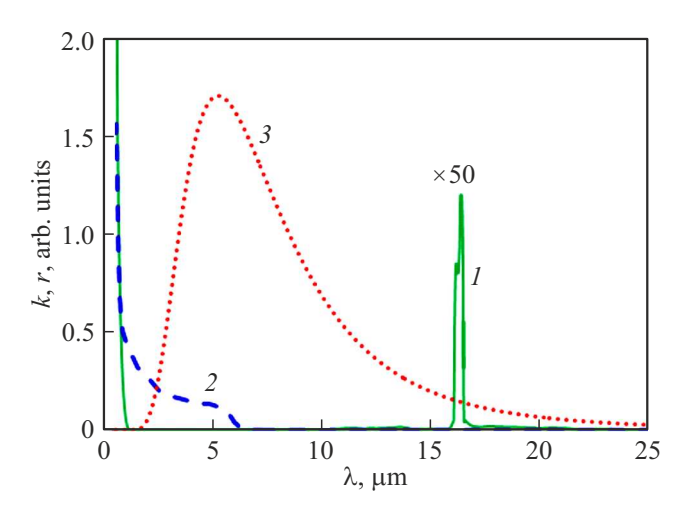


**Figure 2.** Absorption spectra of silicon (1 — multiplied by 50) and CdHgTe x = 0.2 (curve 2). Curve 3 is the Planck's function in conventional units for heater temperature of  $T_G = 550 \,\mathrm{K}$ .

# Calculation of the equilibrium temperature

The thermal balance is disrupted when the CdHgTe layer appears on the Si/CdTe substrate, since in addition to phonon absorption of radiation in silicon, a fundamental absorption region of CdHgTe is added. Figure 3 shows the spectral density curves of radiation absorbed by the Si/CdTe/Hg<sub>0.8</sub>Cd<sub>0.2</sub>Te structure per unit of time from the heater  $\varepsilon(\lambda)$ . The curves are calculated for different values of layer thickness CdHgTe as a product of the Planck function and absorption capacity.

The total flux of absorbed radiation energy from the heater is obtained by integrating the spectral density of the absorbed radiation over the spectral range under In addition, the radiation flux from the consideration. chamber should be added, but it is significantly less, since the temperature of the chamber background was assumed to be 300 K. Therefore, taking into account the chamber radiation will not change the qualitative picture.

The contribution to the total heat flux from intrinsic absorption of CdHgTe increases with the increase of the thickness of CdHgTe layer, which is represented in Figure 3 by spectral density curves  $\varepsilon(\lambda)$  in the region of  $2-6\,\mu\text{m}$ . At a fixed thickness, the equilibrium temperature of the sample  $T_s$ , determined by equation (1), will be established after some time. By calculating the thermal energy flux from the external background of the chamber and the fluxes from the substrate in a similar way and numerically solving equation (1), it is possible to determine the equilibrium temperature of the substrate  $T_s$ . The dependence of  $T_s$ on the thickness of the CdHgTe layer found in this way is shown in Figure 4.

As follows from these calculations, the equilibrium temperature increases markedly with the appearance of the layer, and this increase amounts to tens of degrees. Such

temperature changes are significant for CdHgTe epitaxy. A simple and clear explanation can be given for the temperature jump obtained in the calculations. Before the growth of CdHgTe begins, an equilibrium temperature is established between the heater, the Si/CdTe structure and the chamber background. The structure is heated mainly due to phonon absorption in the region of  $\lambda > 10 \,\mu\text{m}$ , since at the considered temperatures the Planck contour in the range of the intrinsic absorption of Si and CdTe

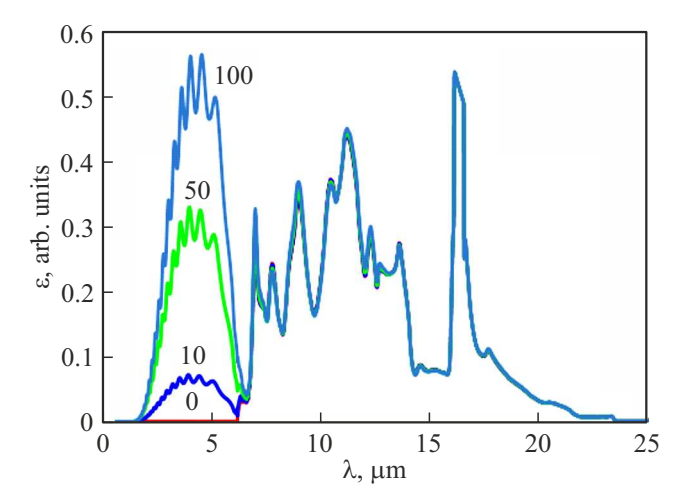
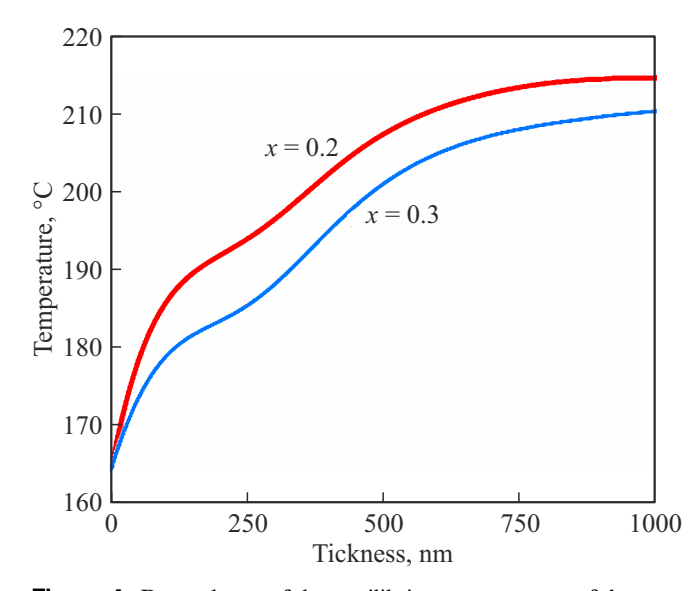


Figure 3. Spectral density of radiation absorbed by the Si/CdTe/Hg<sub>0.8</sub>Cd<sub>0.2</sub>Te structure from the heater (in conditional units). The numbers near the curves correspond to the thickness of CdHgTe layer in nm. Heater temperature is 550 K, CdTe layer thickness is  $6 \mu m$ .



**Figure 4.** Dependence of the equilibrium temperature of the sample on the thickness of the layer CdHgTe in the Si/CdTe/CdHgTe structure, calculated for two values of composition CdHgTe x = 0.2 and 0.3 (shown in the figure). The thickness of the CdTe layer and the temperature of the heater are the same as in Figure 3. The temperature of the sample before the start of growth was 165 °C.

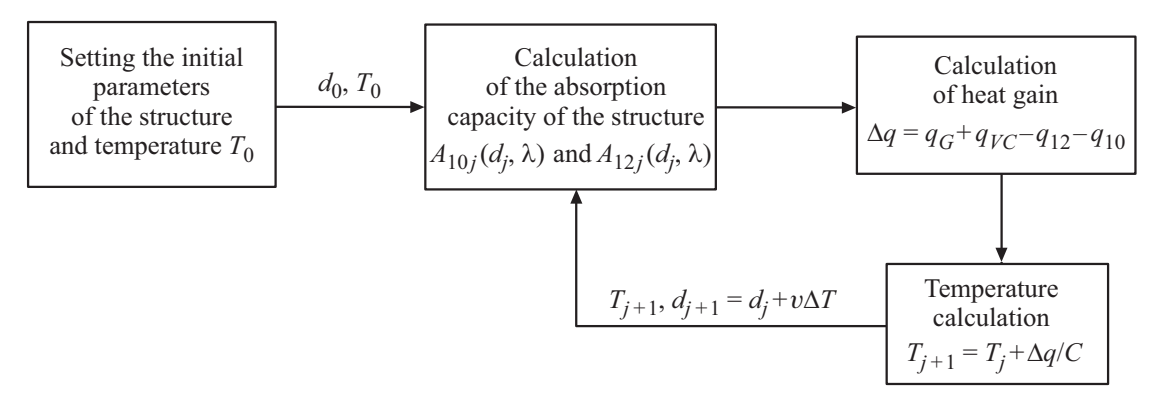


Figure 5. A flowchart for calculating the dynamics of temperature changes.

 $(\lambda < 1\,\mu\mathrm{m})$  is by 6–9 orders of magnitude less than in the region of  $10-20\,\mu\mathrm{m}$ . In this case, the heat flux is proportional to the temperature in the long-wavelength phonon absorption according to the Rayleigh-Jeans law. As a result, the sample temperature is set as the arithmetic mean between the heater temperature and the background temperature. With the appearance of the CdHgTe layer significant part of the heat flux falls on the area of its fundamental absorption in the short-wavelength part of the spectrum of  $2-6\,\mu\mathrm{m}$ . In this spectral region, the heat flux is exponentially proportional to -1/T, so the temperature of the sample is "brought up" to the temperature of a more heated body, i. e., the heater.

# 4. Dynamics of temperature change in the process of growth CdHgTe

Let's estimate the characteristic relaxation time of temperature. The dynamics of temperature changes is described by the equation

$$C\frac{dT_S}{dt} = J_Q, (3)$$

where C is the heat capacity of the substrate surface unit,  $J_Q$  is the balance of absorbed and radiated thermal energy power for the surface unit. Let's represent the substrate temperature as the sum of the equilibrium temperature for a given layer thickness  $T_b$  and the variable component:  $T_S = T_b + T(t)$ . Assuming that the emissivity of the surfaces is equal and constant within the Planck contour  $(A_{10} = A_{12} = A)$  and neglecting the background radiation, we can write

$$J_{Q} = \sigma A \left[ T_{G}^{4} - 2 \left( T_{P} + T(t) \right)^{4} \right] \approx -8\sigma A T_{b}^{3} T(t), \qquad (4)$$

where  $\sigma$  is the Stefan-Boltzmann constant. Here we took advantage of the smallness of  $T(t) \ll T_b$  and the condition that at equilibrium temperature  $J_Q = T_G^4 - 2T_b^4 = 0$ , therefore  $T_b = T_G/\sqrt[4]{2}$ . Taking into account (4) the equation (3) is simplified:  $C\frac{dT(t)}{dt} = -\sigma A8T_b^3T(t)$ , and its solution can be represented as  $T(t) = \mathrm{const} \cdot \exp(-t/\tau)$ , where the time

constant is  $\tau = \frac{C}{(4\sqrt[4]{2}A\sigma T_G^3}$ . Calculations show that the emissivity of the structure is  $A \approx 0.1$ , and then we get  $\tau \approx 180 \,\mathrm{s}$ . Thus, at a growth rate of  $v = 1 \,\mathrm{nm/s}$ , the characteristic temperature relaxation time of the sample is comparable to the growth time of a film with a thickness This means that in order to correctly of  $\sim 100$  nm. determine the temperature dependence, it is necessary to take into account the continuous change in thickness. Such calculations were carried out numerically. Figure 5 shows the calculation algorithm. The absorption capacities of  $A_{12}$  and  $A_{10}$  were calculated as functions of wavelength and layer thickness. When calculating the heat increment, the integration was carried out in the spectral range from 500 nm to  $25 \mu m$ , capturing the phonon absorption region of silicon. After calculating the temperature on the jth cycle, the layer thickness for the j+1st cycle was increased by  $v\Delta t$  and the calculation was repeated. Time step  $\Delta t = 1$  s, growth rate of CdHgTe layer v = 1 nm/s. After the thickness reached its final value, the cycles were repeated at a fixed thickness value.

Figure 6 shows the calculated dynamics of temperature changes during the growth of the CdHgTe layer and

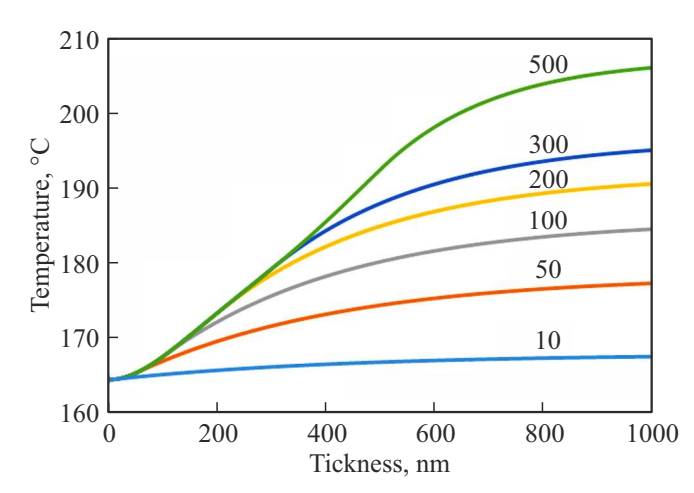


**Figure 6.** The dynamics of temperature changes with the growth of CdHgTe layer x = 0.2. The numbers near the curves show the thickness of the grown film in nanometers.

The residual change of the temperature after completion of growth of CdHgTe layer

d, nm	10	50	100	200	300	500
$\Delta T$ , °C	1.9	7.7	11.2	12.0	12.5	14.1

after its completion. Taking into account that the growth rate was assumed to be 1 nm/s, the end time of growth (in seconds) numerically coincides with the layer thickness (in nanometers). First, the temperature changes with the thickness, and after the thickness reaches the final value (indicated by the numbers next to each curve), the temperature relaxes to its equilibrium value. For instance, the growth stops at 100th second for a curve with the number 100, it stops at 200th second for a curve with the number 200 and so on. The residual temperature change after the end of growth is shown in the table. The values of temperature changes obtained in these calculations seem to be quite significant, and they can be detected experimentally.

# Experiment modeling, results, and discussion

The calculations performed show that in the case of radiative heat transfer, a noticeable increase in temperature should be observed with the beginning of an increase in CdHgTe. In principle, this increase can be detected using ellipsometric measurements. However, the difficulty of the ellipsometric experiment lies in the fact that with the beginning of layer growth CdHgTe shows sharp changes in ellipsometric parameters due to interference on the layer. These changes are several orders of magnitude higher than those that could potentially be related to temperature. The results shown in the table show, however, that temperature changes will be observed even after the cessation of growth. It follows from the data in the table that, for experimental verification of the effect, it is desirable that the thickness of the grown layer be greater 50 nm. Then the expected temperature increase will be  $\sim 10^{\circ}$ , and it can be detected experimentally.

Various ellipsometric temperature control techniques in CdHgTe MBE technology are considered in Ref. [5]. The interference technique based on recording the displacement of interference oscillations of ellipsometric parameters occurring on the CdTe buffer layer in the transparency region of the material ( $\lambda > 850\,\mathrm{nm}$ ) is most suitable to detect the effect described above. This technique has a high sensitivity due to the large thickness of the CdTe layer. The presence of CdHgTe layer shields the penetration of light, and the amplitude of interference oscillations decreases with the increase of CdHgTe thickness, which reduces the accuracy of measurements. Therefore, the thickness of CdHgTe layer was chosen in the range of 50–100 nm.

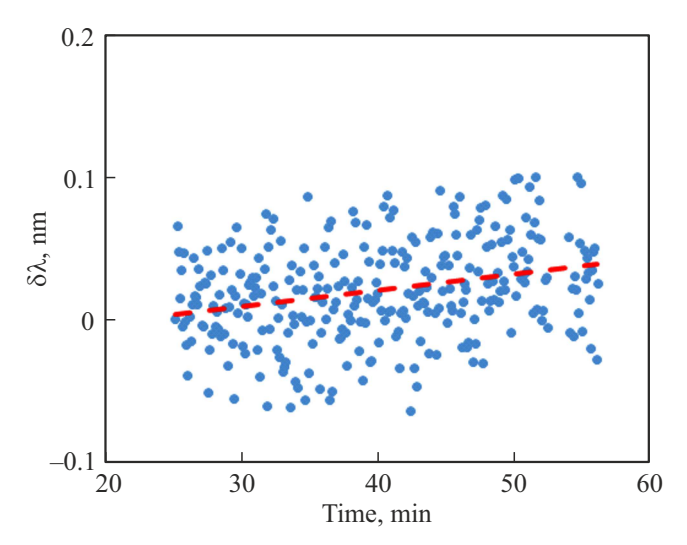


**Figure 7.** The shift of the interference oscillations of the axis parameter after completion of the growth of CdHgTe layer. The dotted line shows the regression line.

The experiment was performed using MBE installation "Ob", equipped with a spectral ellipsometer operating in the wavelength range from 350 to 1000 nm. position of the interference oscillations was continuously monitored throughout the experiment. Before the start of the CdHgTe growth, the epitaxy module was maintained for a sufficient time for the temperature to stabilize. Then a flap was opened, shielding the sample from heated sources of cadmium and mercury. This led to a slight shift in the interference oscillations due to the heating of the sample. After 8-10 min, when the ellipsometric spectra stabilized, a layer of CdHgTe composition close to 0.2 was grown for 1 min. The thickness of the grown layer was  $\sim 60\,\mathrm{nm}$  according to ellipsometry data. The growth was carried out in a constant heater power mode to ensure a constant temperature of the graphite washer  $T_G$ . During the growth process, the transformation of the spectra of ellipsometric parameters was observed, which were caused by a change in the thickness of the layer. After the growth stopped, the position of interference oscillations stabilized. Only the first spectrum  $\Psi(\lambda)$ , measured 8 s after the completion of the growth, had a shift along the axis  $\Psi$ , apparently due to the formation of the CdTe surface layer [16]. It is estimated that the thickness of this layer may be 0.5 nm. No changes in the spectra of the ellipsometric parameters were detected during subsequent measurements. Figure 7 shows the spectral shift  $\delta\lambda$ of one of the maxima of the parameter fluctuations  $\Psi$ , measured within 30 min after the completion of the growth of CdHgTe. The shift is calculated relative to the first measurement. In terms of temperature (a shift of 1 nm corresponds to a temperature change of 17 °C) the average temperature change in 30 min did not exceed 0.7 °C with a data spread of  $\pm 1\,^{\circ}\text{C}$ . The temperature change was also within one degree in a repeated experiment. The results

obtained show that under conditions of mechanical contact between the sample and the graphite washer, thermal radiation is not the dominant heating mechanism of the sample.

An alternative heat transfer option was also considered due to the thermal conductivity of mercury vapor, the pressure of which in the chamber was measured by a sensor and was  $P = 2 \cdot 10^{-2} \, \text{Pa}$ . In this case, the heat flux density between the sample and the graphite washer is easily calculated in the rarefied gas approximation and expressed by the ratio  $j_Q = \sqrt{\frac{R}{\mu}} \left( \frac{P(T_G - T_S)}{\sqrt{T_G} + \sqrt{T_S}} \right)$ . Here  $\mu$  is the molar mass of mercury, R is the universal gas constant. For the substrate and washer temperatures of  $T_S = 440 \,\mathrm{K}$ and  $T_G = 500 \,\mathrm{K}$ , we obtain that the heat flux density will be  $J_Q = 18 \,\mu\text{W/cm}^2$ . At the same time, the density of heat actually absorbed by the structure, estimated based on the heating rate of the plate when entering the growth mode, was  $\geq 12 \,\mathrm{mW/cm^2}$ . Thus, the option of heat transfer by mercury molecules turns out to be untenable. Most likely, the dominant heating mechanism is the thermal conductivity between the sample and the graphite washer, as well as between the sample and the holder. Being a relatively soft material, graphite can provide a large contact area and a fairly good thermal contact due to plastic deformation.

#### 6. Conclusion

The study considers the influence of the growing epitaxial layer of CdHgTe on the established thermal balance between the heater (graphite washer) and the substrate in conditions where heat exchange occurs only due to thermal radiation. Numerical calculations have been performed and it is shown that when a CdHgTe layer appears the thermal balance is disrupted, and this leads to an increase in temperature, which can reach several tens of degrees. The calculated dynamics of temperature changes shows that an increase in temperature will also be observed after the layer stops growing. The experiments made it possible to establish that in installations of type "Ob", when the sample is pressed against the holder with a heated graphite washer, the radiative heating mechanism is not dominant.

#### **Funding**

The work was performed within the framework of the state assignment of the Ministry of Science and Higher Education of the Russian Federation, project FWGW-2025-0008.

### **Conflict of interest**

The authors declare that they have no conflict of interest.

#### References

- J.W. Garland, S. Sivananthan. *Molecular-Beam Epitaxial Growth of HgCdTe*.
  G. Dhanaraj, K. Byrappa, V. Prasad, M. Dudley (eds). *Springer Handbook of Crystal Growth* (Springer, 2010) p. 1069]. DOI: 10.1007/978-3-540-74761-1
- [2] J. Garland. MBE Growth of Mercury Cadmium Telluride in: P. Capper, J. Garland (eds). Mercury Cadmium Telluride: Growth, Properties Applications (Wiley, Hoboken, 2011) p. 131). https://doi.org/10.1002/9780470669464.ch7
- [3] J.A. Roth, T.J. de Lyon, M.E. Adel. Mater. Res. Soc. Symp. Proc., 324, 353 (1994). https://doi.org/10.1557/PROC-324-353
- [4] M. Daraselia, C.H. Grein, S. Rujirawat, B. Yang, S. Sivananthan, F. Aqariden, H.D. Shih. J. Electron. Mater., 28, 743 (1999). DOI: 10.1007/s11664-999-0064-4
- [5] V.A. Shvets, D.V. Marin, I.A. Azarov, M.V. Yakushev, S.V. Rykhlitskii. J. Cryst. Growth, 599, 126898 (2022). https://doi.org/10.1016/j.jcrysgro.2022.126898
- [6] L.A. Almeida, N.K. Dhar, M. Martinka, J.H. Dinan. J. Electron. Mater., 29, 754 (2000).DOI: 10.1007/s11664-000-0220-3
- [7] R. Schlereth, J. Hajer, L. F.rst, S. Schreyeck, H. Buhmann, L.W. Molenkamp. J. Cryst. Growth, 537, 125602 (2020). https://doi.org/10.1016/j.jcrysgro.2020.125602
- [8] T.J. De Lyon, R.D. Rajavel, J.A. Roth, J.E. Jensen. In: *Hand-book of Infra-red Detection Technologies*, ed. by M. Henini and M. Razegh (Elsevier Science, 2002) p. 309.
- [9] V.A. Shvets, D.V. Marin, I.A. Azarov, M.V. Yakushev, S.V. Rykhlitsky. FTP, 55 (12), 1240 (2021). (in Russian). DOI: 10.21883/FTP.2021.12.51713.9714
- [10] I.A. Azarov, V.A. Shvets, S.A. Dulin, N.N. Mikhailov, S.A. Dvoretskii, D.G. Ikusov, I.N. Uzhakov, S.V. Rykhlitskii. Avtometriya, 53 (6), 111 (2017). (in Russian). DOI: 10.15372/AUT20170614
- [11] J.M. Palmer, B.G. Grant. Art of radiometry (SPIE P.O. Box 10 Bellingham, Washington 98227-0010 USA, 2010).
- [12] R. Azzam, N. Bashara. Ellipsometriya i polyarizovannyj svet (M., Mir, 1981) p. 379. (in Russian).
- [13] Handbook of Optical constants of Solids, ed. by Edvard D. Palik (Academic Press, 1998).
- [14] S. Adachi. Optical constants of crystalline and amorphous semiconductors. Numerical data and graphical information (Kluwer Academic Publishers, 1999).
- [15] J.P. Laurenti, J. Camassel, A. Bouhemadou, B. Toulouse, R. Legros, A. Lusson. J. Appl. Phys., 67, 6454 (1990). DOI: 10.1063/1.345119
- [16] V.A. Shvets, D.V. Marin, M.V. Yakushev, S.V. Rykhlitsky. Opt. i spektr., 129 (1), 33 (2021). (in Russian). DOI: 10.21883/OS.2021.01.50436.213-20

Translated by A.Akhtyamov